
Article:
Maiti, R. and Mills, R. (2017) Wear Properties of Diamond-like-carbon coatings with Silicon and Chromium as adhesion layer using a High Frequency Reciprocating Rig. Proceedings of the Institution of Mechanical Engineers Part J-Journal of Engineering Tribology, 231 (12). pp. 1605-1615. ISSN 1350-6501

https://doi.org/10.1177/0123456789123456

Wear Properties of Diamond-like-carbon coatings with Silicon and Chromium as adhesion layer using a High Frequency Reciprocating Rig

Raman Maiti[1]*, Robin Mills[1]

[1]Department of Mechanical Engineering, Sir Frederick Mappin Building, University of Sheffield, Sheffield

S13JD, UK

* Corresponding Author

Raman **Maiti**

Department of Mechanical Engineering,

Sir Frederick Mappin Building,

University of Sheffield,

Sheffield S13JD, UK

Email: r.maiti@sheffield.ac.uk

Tel: +44 (0) 114 222 7805

Fax: +44 (0) 114 222 7890

Abstract

The application of Diamond-like-carbon coatings (DLC) to bearing surfaces is widespread from machining to bio-implants and has resulted in significant study of coating properties. The aim of this investigation was to determine the performance of two diamond-like-carbon coatings, using Chromium and Silicon as adhesion layers. Linear reciprocating wear tests were carried out at room temperature using an AISI 440C steel ball reciprocating against the DLC coated metal substrate. The performance of the coatings under different contact pressures (500 to 3000 MPa); peak sliding velocities (28 to 378 mm/s); and stroke length, (1.5 to 4 mm). An electric resistance measurement was used to monitor coating failure owing to the dielectric nature of the tested coatings.

An increase in contact pressure resulted in a decrease in number of cycles to failure for both the coatings. However, the number of cycles to failure increased proportionally with sliding speed. In addition, artifacts on the coating and blister formation generated coating debris which acted as a third body during the wear process. The debris caused complete delamination of the coatings initially at the ends of the wear scar. The Silicon adhesion layer coating samples were found to provide a greater resistance to failure due to it being thicker, harder, and more elastic as compared to samples having a Chromium adhesion layer.

Keywords: wear, diamond-like-carbon coating, failure cycles, high frequency reciprocating rig; adhesion layer

1. Introduction

Diamond-like-carbon (DLC) coatings consist of amorphous or hydrogenated amorphous carbon consisting mainly of sp^3 and sp^2 hybridised Carbon atoms, similarly found in diamond and graphite respectively. They have a wide range of applications from machining to bio-implants as its hardness may approach half that of diamond (sp^3 Carbon-Carbon bonding) (1-6). Previous investigators working with DLC have reported wear performance of the DLC coatings using pin-on-disc, ball-cratering, reciprocating ball-on-plate and ring-on-disc apparatus (7-10). Results have shown large variations in the wear properties owing to different deposition techniques, coating thickness above adhesion layer, type of metal substrate and experimental conditions (8, 11). Buchner et al. (11) also reported that the material and chemical properties of DLC coatings can be tailored by controlling the composition and deposition techniques utilised. Details of which can be found in studies such as Bull (12) and Dearnley et al. (13).

DLC has been deposited on many different substrate materials. Examples include Cobalt-Chromium alloys (14-18), Titanium alloys (19), stainless steels (2, 20, 21) and more recently ultra-high molecular weight polyethylene (22, 23). Significant reductions in wear rates have been observed in cases of DLC coated metallic and non-metallic substrates. However, the majority of the failures were due to the generation of high internal residual stress between the coating and substrate surfaces resulting in coating delamination (1, 3, 6, 24-28). Many authors (1, 3, 6, 24, 25) have focused on reducing delamination by adding an adhesion layer such as Silicon (Si), Titanium (Ti), Aluminium (Al) and Chromium (Cr). These adhesion layers create a transition between the substrate and the coating which reduces the likelywood of delamination (1, 3, 6, 24, 25).

In this study, adhesion layers of Chromium and Silicon are used to determine their relative benefits at improving the wear resistance of DLC on a EN31 steel substrate. Specimen with adhesion layers of different thickness, hardness and elastic modulus were tested under a range of contact pressures (500 to 3000 MPa) and peak sliding-velocities (28 to 378 mm/s).

2. Materials and Methods

2.1 Specimens and their properties

The DLC coated steel with Silicon and Chromium adhesion layers will be denoted as coating A (Si+a-C:H) and coating B (Cr+a-C:H). The composition and the material properties of each coating are detailed in Table 1. The average roughness (Ra) of the coated specimen before the test was 0.10 µm.

Table 1: Test material properties (26).

Material	**Coating A**	**Coating B**	**Steel (Substrate)**	**Steel (Ball)**
Chemical composition	Si+a-C:H	Cr+a-C:H	EN 31	AISI 440C
Thickness (µm)	4	1.7	-	-
Young's modulus (GPa)	222	111	210	210
Hardness (GPa)	23	12	0.3	0.7
Poisson's ratio			0.3	0.3

Coating A (Si+a-C:H)

Coating A is an amorphous based standard hydrogenated DLC coating with a Silicon as an adhesion layer (Tecvac Ltd, Cambridgeshire). The DLC coating of maximum thickness of 4 µm, was deposited on the metal substrate by plasma-

enhanced Chemical Vapor Deposition (CVD), using a mixture of acetylene (C_2H_2) and teramethylsilane as the material gas. A hardness of 23 GPa and a Young's modulus of 222 GPa was provided by the manufacturer.

Coating B (Cr+a-C:H)

Coating B was another type of amorphous based hydrogenated DLC coating (Dymon) with a Chromium adhesion layer (Teer Coatings Ltd, Worcestershire). Deposition was by magnetron sputtering of Cr target (99.99%) and a linear ion source supplied with CH_4 precursor gas. The coating had a thickness of 1.7 μm. A hardness of 12 GPa and Young's modulus of 111 GPa was provided by the manufacturer.

Steel ball and substrate specimens

The ball specimens articulating against the DLC coating and the substrate specimen were made of AISI 440C and EN31 steel respectively. The ball specimens were electrically coupled to the holder.

2.2 Specimen preparation

In order to reduce the effect of foreign particles during the test and enable calculation of the exact volume of wear scar, all specimen were ultrasonically cleaned with isopropanol before and after the test.

2.3 Test Rig

The high frequency reciprocating (HFR) used under dry friction conditions at standard room temperature (20±2 ^{o}C) and humidity (70%), is shown in Figure 1.

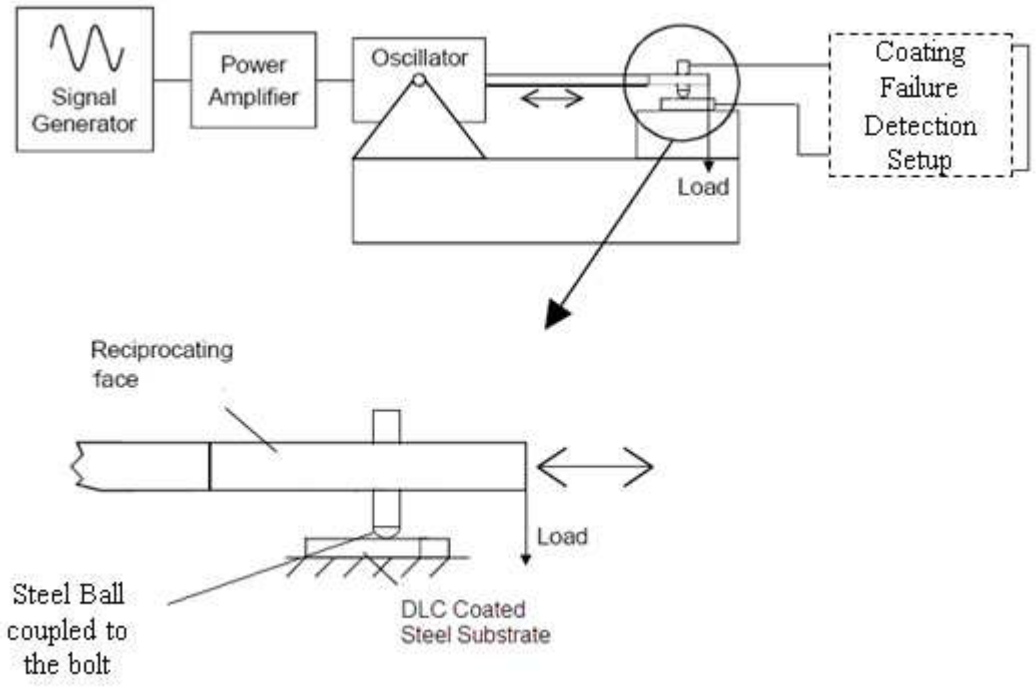

Figure 1 Schematic diagram of high frequency reciprocating test rig.

The driving apparatus consisted of a signal generator, power amplifier, linear motor, specimen mounting, loading unit and a resistive coating failure detection circuit. The signal generator was used to set the reciprocation parameters, namely peak velocity and the power amplifier drove the linear motor. The ball specimen was mounted to the reciprocating stem of the linear motor. Dead weight loading was applied through the load application wire at the end of the reciprocating stem. During the testing, the AISI 440C balls slid over the DLC specimens at frequencies ranging from 5 to 30 Hz, equivalent to peak sliding-velocities ranging from 28 to 378 mm/s. A maximum Hertz contact pressure ranging from 0.5 to 3 GPa was obtained using balls of diameters 2-15mm under no lubrication. The stroke length varied from 1.5 to 4 mm, controlled by the application of constant load.

Ball-on-flat and pin-on-flat configurations do not have the same tribological behaviour. Due to the flat surface of the pin in the pin-on-flat apparatus, the surface

area is higher compared to the ball on flat apparatus. However, the presence of asperities on the flat surface results in a lower surface area and hence, higher contact pressure based on Hertz contact theory (2). This is not the case for contact in ball on flat (i.e. HFR rig in the current study), where the surface area in contact was based on the contact of the ball and therefore as the area was reduced, the presence of asperities was lower. The ball diameter and load applied for the test generated the required maximum contact pressure based on Hertz contact theory (2). Hence in this study, a ball on flat apparatus was preferred. During sliding however, the contact of the ball gradually increased from a point to a surface contact. But this effect can be assumed to be negligible as the ball was changed in every test.

The applied load, *W*, and ball diameter, *D*, were varied to obtain the desired maximum Hertz contact pressure, P_{max}, in the HFR contact configuration. P_{max} was calculated using Equation (1) (29)

$$\mathrm{P_{max}} = \frac{3}{2}\mathrm{P_{mean}} = \frac{6\mathrm{W}}{\pi \mathrm{a}^2}, \qquad (1)$$

where *a* is the diameter of the contact area and $\mathrm{P_{mean}}$ is the mean Hertz contact pressure. The diameter of contact was determined from the applied load and ball's diameter by Equation (2)

$$\mathrm{a} = \frac{3\,\mathrm{k}\,\mathrm{D}\,\mathrm{W}}{8\,\mathrm{E_2}}, \qquad (2)$$

where *k* is the modified Young's modulus coefficient and is given by Equation (3)

$$\mathrm{k} = (1-\upsilon_2^2) - (1-\upsilon_1^2)\frac{\mathrm{E_2}}{\mathrm{E_1}}. \qquad (3)$$

The constant *k* is evaluated from material properties of the ball (subscript 1) and disc (subscript 2), namely the Young's modulus, *E*, and the Poisson ratio, *v*.

2.4 Coating failure detection

In order to quantify the longevity of the DLC coatings, it was necessary to compare the number of cycles to failure for each of the coatings. The resistance circuit used to determine coating failure was based on that used in the computerized Micro-Tribometer UMT-2 (30). According to previous investigators (31, 32), a coating resistance of 10^8 Ohm cm^{-1} was observed even at a thickness of 3 nm. Hence, the technique which uses the dielectric properties of DLC is effective even when close to coating break-through. The electrical contact circuit facilitating the detection of failure cycles for the coating is shown in Figure 2. The circuit consisted of an analogue to digital converter (ADC), DC voltage source (9V battery), a steel ball and a DLC coated metal substrate. Maximum, mean and minimum voltage plots were recorded and plotted using LabVIEW (National Instrument Corporation, Newbury, UK). Initially the DLC coating behaved as an open circuit with no current flow owing to its dielectric properties. At the onset of coating penetration, a jump in the voltage equal to the supply voltage was observed (Figure 3: failure of Cr+a-C:H DLC coating at 30 Hz and 750 MPa contact pressure), signifying the failure of the DLC coating. The failure of the coating effectively created a short between the ball and the specimen substrate and hence, the voltage jump was observed. The number of cycles to failure was determined by the identification of this voltage jump. The onset of failure was recorded when the constant maximum voltage is attained to avoid errors in failure detection.

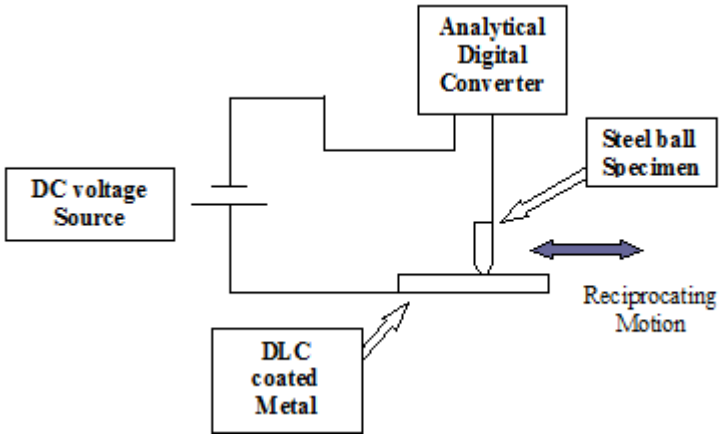

Figure 2 Contact circuit for DLC coating failure detection.

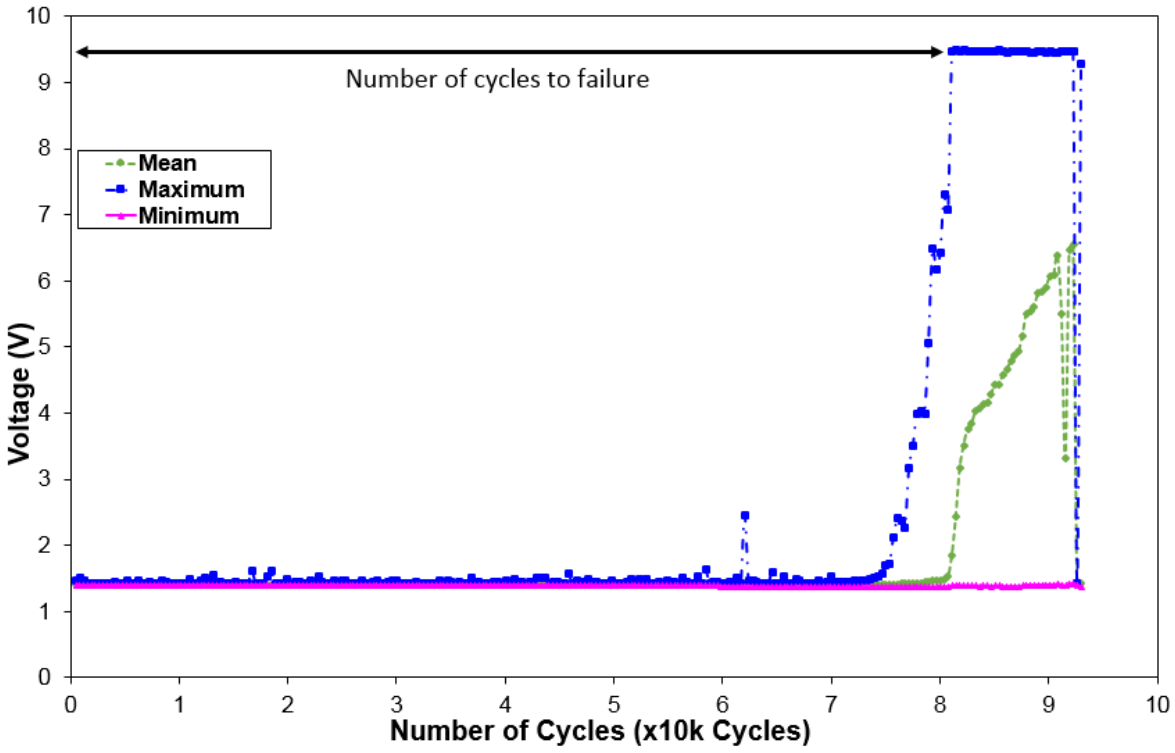

Figure 3 Typical jump in voltage upon coating failure for Cr+a-C:H DLC coating at 750 MPa contact pressure and 30 Hz frequency.

Due to variation in the thickness and hardness, the coatings were compared for longevity based on the number of cycles to failure per unit hardness per unit thickness (NCF) plotted against variation in pressure and peak sliding velocity. As

no information on the thickness of individual layers (a-C:H coating and adhesion layers) was provided by the supplier, the total thickness was used for the calculation of NCF. Each test condition was performed twice on the same day to avoid environmental conditions affecting repeatability.

2.5 Estimation of wear rate coefficient

Generally the measurement of weight loss is calculated using gravimetric measurement (2, 26). However, in the present study due to significantly small volumetric wear, this method of measurement was deemed not capable of providing accurate results. Hence the volumetric wear was determined by measuring the wear scar dimensions (Figures 4 and 5) using an Inform Talysurf profilometer (Taylor Hobson, Philadelphia, USA).

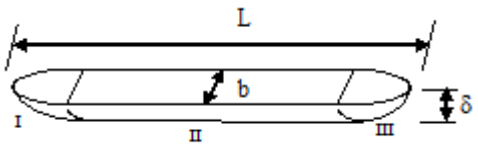

Figure 4 Dimensions of wear scar.

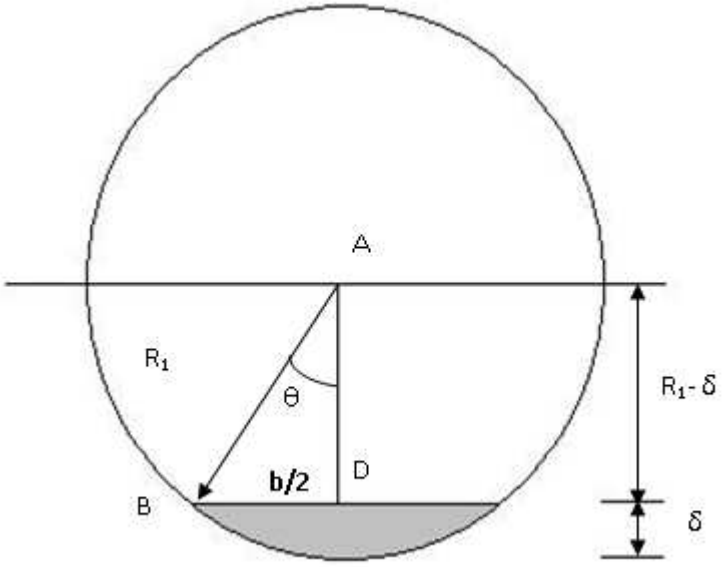

Figure 5 Material removed by spherical ball shown in 'grey' colour.

The volume of the scar (V_{ws}) was the sum of three volumes as shown in Figure 4 and calculated by the Equation (4)

$$V_{ws} = V_I + V_{II} + V_{III} \qquad (4)$$

V_I , V_{III} are calculated by the Equation (5) and V_{II} is expressed by the Equation (6)

$$V_I = V_{III} = \frac{\pi}{12}[3(\frac{b}{2})^2 + \delta^2]\delta \qquad (5)$$

$$V_{II} = A(L - b) \qquad (6)$$

where, A is the area of the cylindrical segment expressed as Equation (7) and b is the width of the scar (Figure 5) expressed by Equation (8)

$$A = \frac{1}{2}R_1^2\theta - (R_1 - \delta)\frac{b}{2} \qquad (7)$$

$$\frac{b}{2} = \sqrt{2R_1\delta} \qquad (8)$$

where, R_1 is the radius of the ball specimen, δ is the total thickness of the DLC inclusive of the adhesion layer above the metal substrate and L is the length of the scar.

The wear coefficient ($WCoeff$) was calculated using Equation (9)

$$WCoeff = \frac{V_{ws}}{2NCF(L-b)W} \qquad (9)$$

where, NCF is the number of cycles to failure ad W is the applied load. The wear coefficient of the coatings was represented as mean ± 95% confidence limit (Pa^{-1}). A two way paired ANOVA post-hoc Student test was performed between the wear coefficient of coating A (with Si as adhesion layer) and coating B (with Cr as adhesion layer) for significance at *p<0.05.

2.6 Graphitisation of DLC coatings

The wear particles (originated from DLC coating) on the reciprocating ball specimen were analysed for graphite content using Thermo Nicolet DXR Raman's Spectroscopy with D and G peaks at 1350 cm^{-1} and 1580 cm^{-1} (3, 33). The wavelength of the spectroscopy was 532 nm with special resolution of 1 µm and confocal depth of 2 µm. Due to the lower intensity, the laser beam did not contribute to the graphitization of DLC. The position of two peaks depicted the presence of either DLC or graphite content when compared to non worn DLC material. However, studies in past by Steiner et al. (33) have observed that graphite content is more relevant at these two peak center independent of the adhesion layer used in the DLC coating substrate.

2.7 High magnification images

Images were taken before and after testing using a Tabletop Scanning Electron Microscope (SEM) TM3030Plus (Hitachi, Schaumburg, USA). The DLC coated substrate was cut along and perpendicular to the scar length to investigate the failure mechanism. Following the cut, the substrates were grinded and polished to a final stage using 15 nm AlO_2 abrasive particles (34).

3. Results

3.1 Number of cycles to failure (NCF)

Typical plots of variation of NCF per unit thickness and hardness with respect to velocity and pressure for coatings A and B are shown in Figure 6. An increase in contact pressure resulted in a decrease of NCF for both coatings. However, an increase in sliding velocity resulted in an increase of NCF. Therefore, the NCF was directly proportional to contact velocity and inversely proportional to contact pressure. For any combination of contact pressures and sliding velocities, the plots also demonstrated a higher NCF for when Silicon was used as an adhesion layer (Figure 6a) as compared to Chromium (Figure 6b). This suggests that a Silicon adhesion layer coating samples show greater resistance to wear when compared to the use of a Chromium adhesion layer DLC coating.

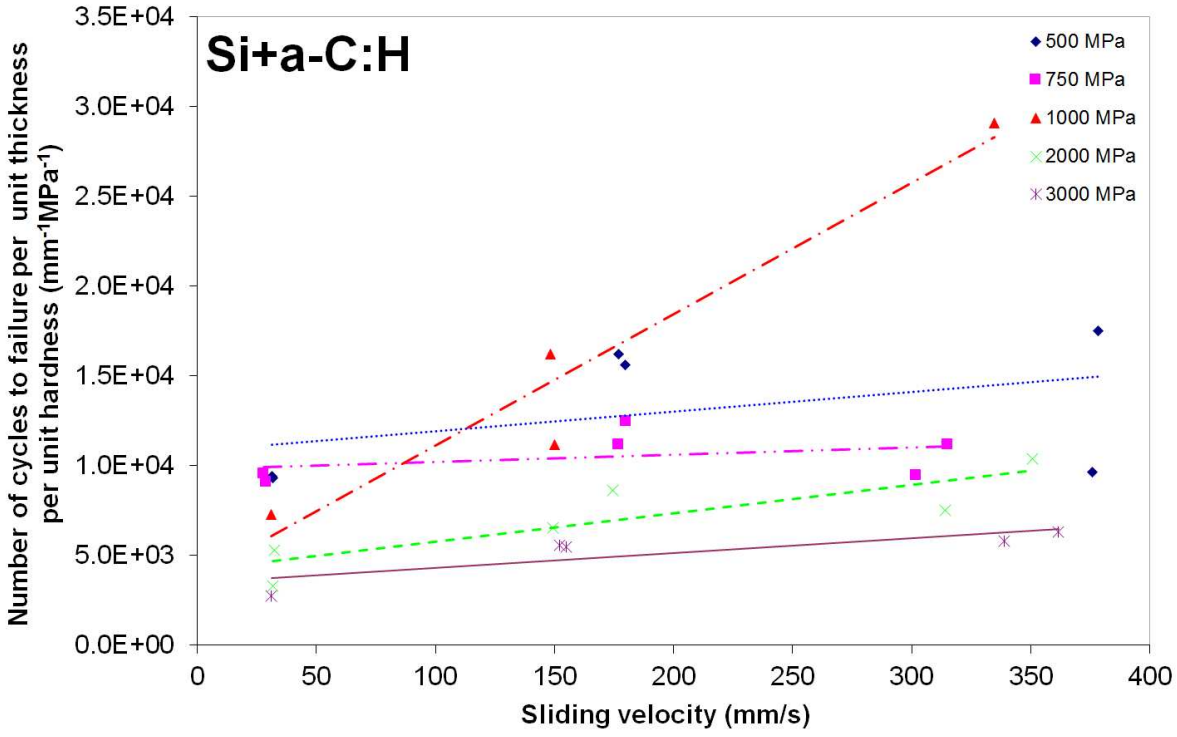

(a) Coating A: Si+a-C:H DLC coating

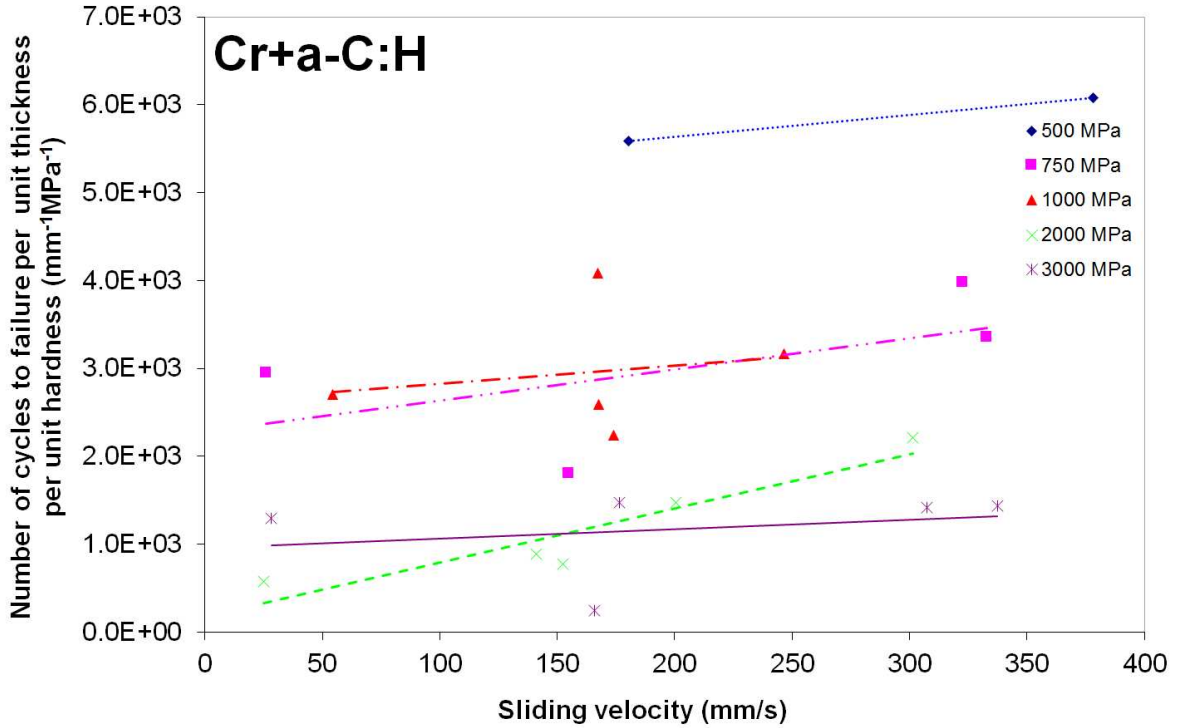

(b) Coating B: Cr+a-C:H DLC coating

Figure 6 Variation in the number of cycles to failure with respect to maximum contact pressure and sliding velocity for (a) Si+a-C:H and (b) Cr+a-C:H DLC coatings.

Higher value of NCF was observed for Coating A at contact pressure (1000 MPa) and highest sliding velocity (335 mm/s). This might be due to high humidity (90%) on the day of testing causing a water lubrication regime between the DLC and steel balls. However, more tests are needed before any conclusion on lubrication regime is made. The second test did not fail even after 0.7 Million cycles. Similarly, for the Chromium adhesion layer, no data points were obtained for the NCF at 500 MPa contact pressure and sliding velocity 28 mm/s (5 Hz frequency). Two separate tests were conducted and neither of the tests showed any signs of coating failures even after 0.7 Million cycles. These results were removed from analysis as the environmental conditions for these tests were different than other tests and the coatings didn't fail after 0.7 Million cycles.

3.2 Wear coefficients

The mean wear coefficient of the Chromium coating B ($9.0x10^{-10}\pm5.1x10^{-10}$ Pa^{-1}) was approximately seven times higher than that of coating A ($1.3x10^{-10}\pm8.3x10^{-11}$ Pa^{-1}). In addition, there was a significant difference between the two wear coefficients ($P<0.01$). The standard deviation of the wear coefficients were high because of the variations in speed, radius of ball and pressure at contact.

3.3 Wear Mechanism

The wear scars for both coatings at 1000 MPa, 500 MPa and 750 MPa contact pressures and 245 mm/s, 180 mm/s and 28 mm/s sliding velocities respectively are shown in Figure 7. This shows that coating penetration initiated at the end of the

wear scar and proceeded towards the centre of the stroke until the coating was completely removed.

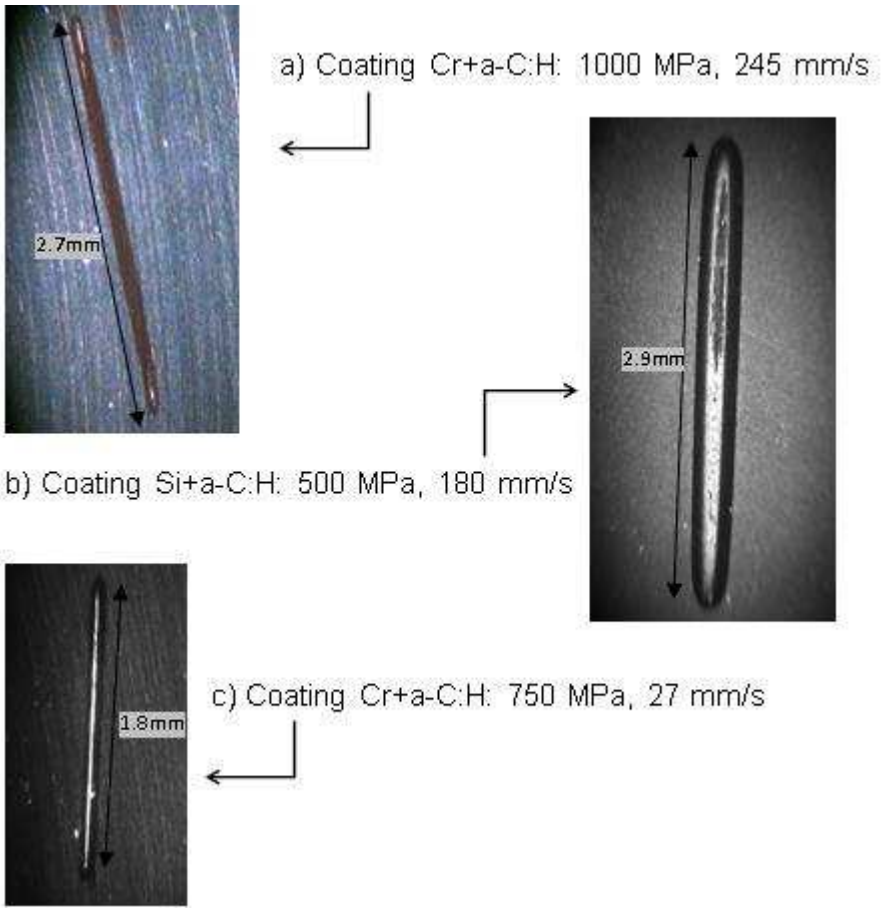

Figure 7 Penetration of DLC coatings evolving at the ends of wear scars to complete coating removal at different pressures and sliding velocities.

4. Discussion

The experiment led to the emergence of five key issues. These are (1) influence of contact pressure on coatings, (2) blister formation, (3) wear debris, (4) transfer of wear debris to ball surface and (5) formation of wear scars.

Contact pressure had an influence on the DLC coating failure. Tests with a higher diameter ball resulted in lower failure rate as compared to the ball with lower diameter. As the contact pressure was higher in the latter configuration, coating

failure occurred at lower number of cycles. Coating A with a Silicon adhesion layer was found to have a higher wear resistance than coating B with Chromium adhesion layer. Coating A had higher coating thickness (2.4 times) and hardness (1.9 times) compared to Coating B which might have resulted in larger number of cycles to failure.

High internal stress generated at the coating/substrate interface due to continuous sliding and high contact pressure is considered to be the major reason for the delamination of the coating and is suggested in work by other researchers (1, 3, 6, 24, 25). It is possible that short length interfacial fractures in the form of blisters have been generated due to cohesion failure and artefacts present in the coated substrate as shown in Figures 8 and 9 (a) respectively (35, 36). Graphite layers were found decapitated from the substrate and stuck to the ball surface as shown in Figures 9 (b), 9 (e) and 9 (f). These chunks might have been removed due to the process of blister formation. The cutting (along X-X axis as shown in Figures 9(c) and (d)), grinding and polishing processes were required to remove the interference of scratches under SEM and observe the blisters in the coating samples. Although these processes were necessary, they might have led to the removal of any blisters. As a result, in the current study, blisters could not be detected under the SEM.

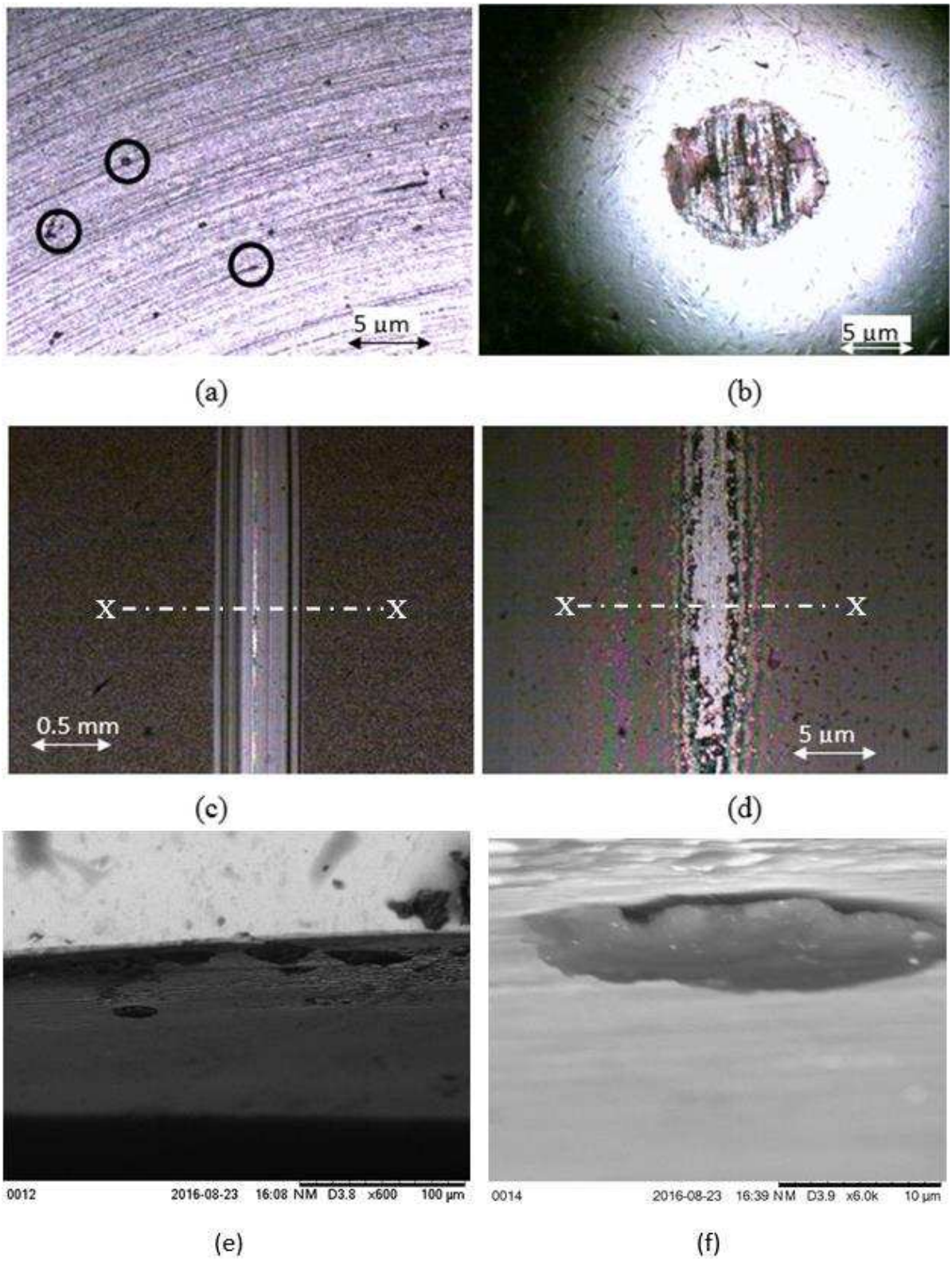

Figure 9 High magnification SEM images of contact surfaces. a) Unworn sections (50x mag) showing surface defects (marked in circles), b) Wear scar of ball (10x mag) showing possible transfer film, Wear track at c) 5x mag and d) 50x mag, layer removal at e) 600x mag and f) 6000x mag of the cut along X-X axis.

Wear products removed from the DLC coating were transferred to the surface if the ball thereby forming a separating layer between the articulating surfaces. Wear particles removed from the ball after testing showed the presence of graphite when analysed using Raman's spectroscopy at G and D peaks (Figure 10). The G bands shifted and D-band emerged into a peak showing graphitisation in the transferred material similar to what was also observed in Suzuki et al. (37). Studies have found that the wear coefficient can be extremely low at this juncture (38) and that graphitization of the DLC coatings plays an important role in the reduction of friction and wear during dry sliding conditions (39-41). The initial contact of metal/DLC quickly results in a layer of graphite being transferred on to the ball which results in a predominantly DLC graphite sliding contact as shown in Figure 9 (b).

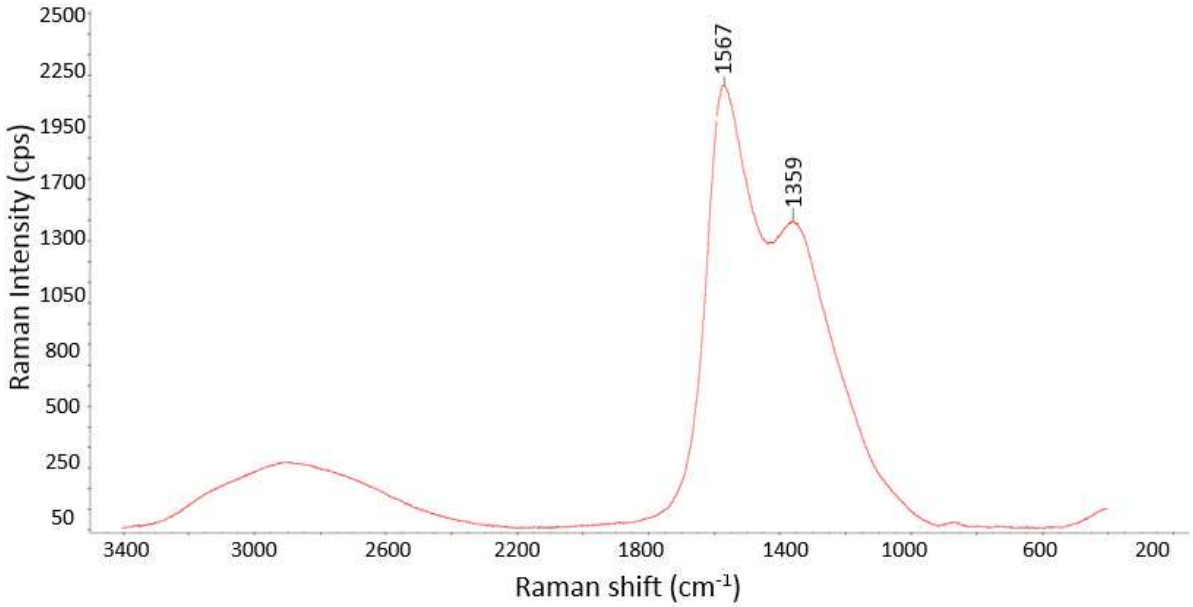

Figure 10 Graphite peak centered at 1350 cm^{-1} and 1580 cm^{-1} analysed using Raman's spectroscopy

In addition to the ball transfer layer, some coating layers fail due to fracture under continuous loading resulting in the formation of debris generated as shown in Figure 9 (c-d). Due to the presence of abrasive wear particles, the scratch marks were mostly found at the ends of the scar as shown in Figure 11. In the presence of third body abrasive wear, coating removal initiated at the ends of the wear scar resulted in the penetration of the DLC coating from the substrate as shown in Figures 7, 11 and 12. The progression from generation of scratches to complete coating failure in the wear scar is shown in Figures 7 and 12 (36).

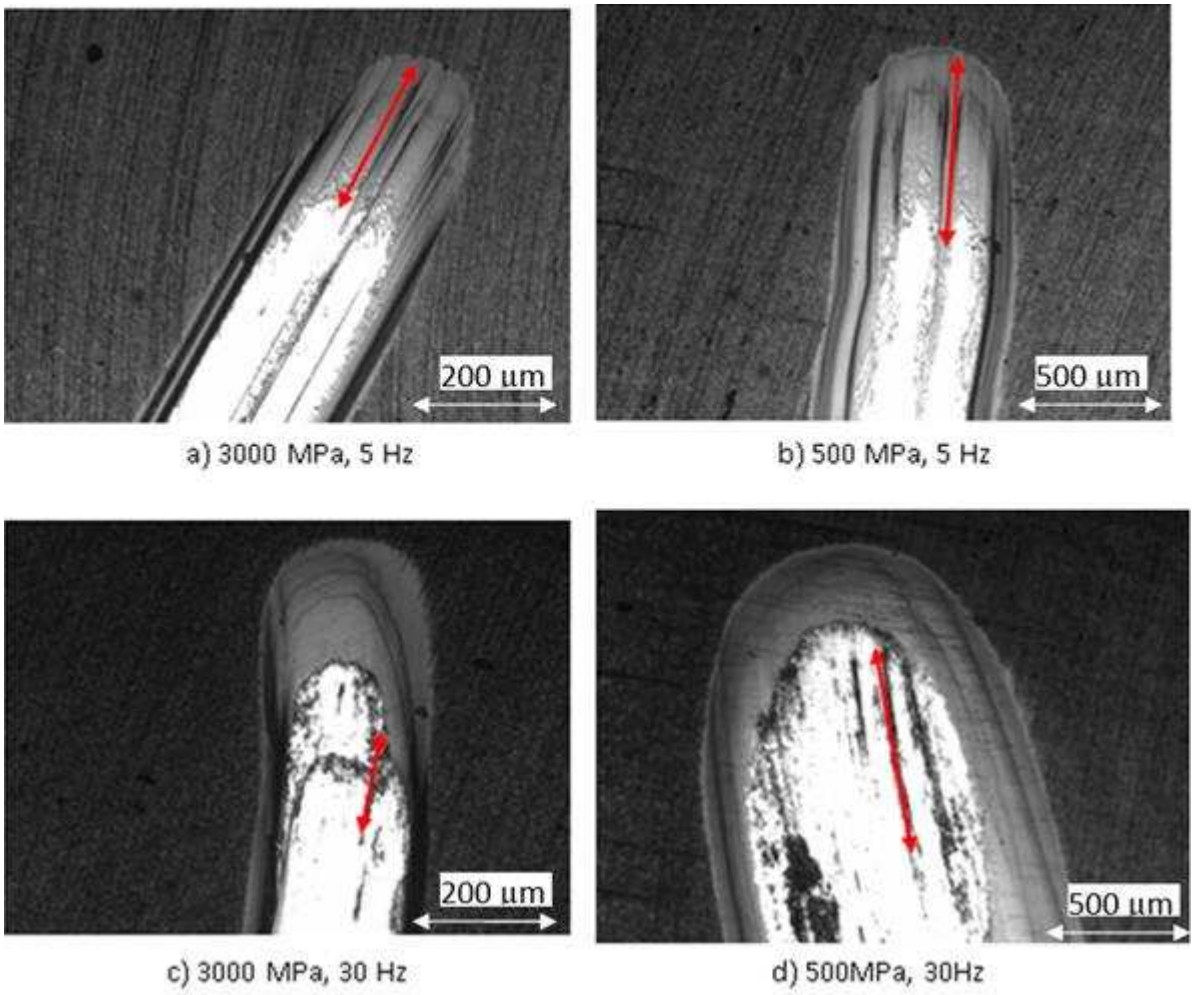

Figure 11 Scratches (marked as arrow) observed at the end of the wear scar.

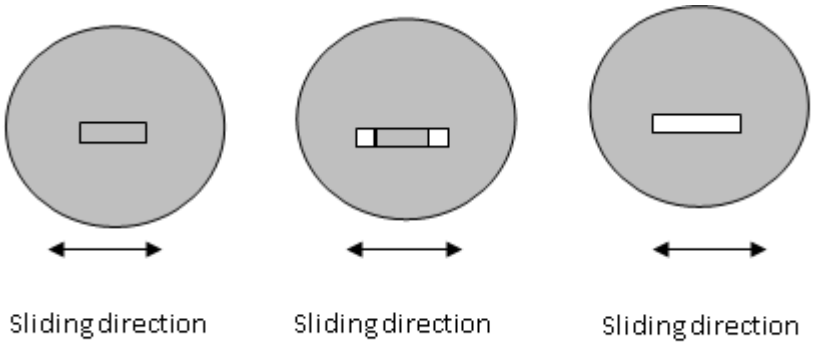

Figure 12 Schematic diagram depicting the progression of micro-delamination and tearing of coating from the substrate (36).

The friction was not quantified in the current study as the tests were carried out to detect penetration failure of DLC coatings which other investigators have considered (10, 36, 38, 42). However, the variation of friction from scratches to complete coating removal should be of great interest and will be investigated in the future. In addition, the coating thickness includes the thickness of adhesion layer. As the adhesion layer is conductive and only DLC coating insulating to the current flow, future studies should exclude the thickness of adhesion layer for the calculation of NCF.

The newly developed method is a novel technique to measure the number of cycles to failure in a DLC coated steel substrate. Future research should investigate the effect of different ball diameters at any contact pressure and effect of external lubrication on the coating failure.

5. Conclusion

This paper examines the wear properties of DLC coatings under dry friction conditions having two different adhesion layers. Amorphous hydrogenated DLC coatings A (Si+a-C:H) and B (Cr+a-C:H) were used for coating failure tests under

varying pressure (500 to 3000 MPa) and speed (28-378 mm/s). A technique based on the insulating properties of the DLC was developed to evaluate the failure of the coatings. This method includes the thickness of electrical conductive adhesion layer. Future studies should exclude this thickness while calculating the number of cycles to failure.

Both pressure and velocity had an effect on the number of failure cycle. An increase in pressure resulted in a decrease in NCF. However, an increase in velocity resulted in an increase in NCF.

Wear debris were generated due to the formation of blisters, artefacts present in the coatings and abrasive wear. This debris acted as third body abrasive particles and therefore resulted in complete removal of the coating initiated from the ends of the wear scar. Silicon adhesion layer was found to provide a greater resistance to failure.

6. Conflict of interest statement

There is no conflict of interest.

7. Acknowledgements

The authors would like to acknowledge Professor Rob Dwyer-Joyce at University of Sheffield for his support during the project.

8. References

1. Hauert, R. An overview on the tribological behavior of diamond like carbon in technical and medical applications. *Tribological International.* 2004; 37: 991-1003.
2. Platon, F, Fournier P, Rouxel S. Tribological behavior of DLC coatings compared to different materials used in hip joint prostheses. *Wear.* 2001; 250: 227-236.
3. Robertson J. Diamond-like amorphous carbon. *Material Science and Engineering R.* 2002; 37: 129-181.
4. Erdemir A, Donnet C. Tribology of diamond, diamond like carbon films. In: Wear – Materials Mechanisms and Practice, Stachowiak, G. W. (Ed.), Tribology in Practice Series, John Wiley and Sons, Chichester, UK, 2005; 191-222.
5. Matthews A, Eskildsen S S. Engineering applications for diamond like carbon. *Diamond and Related Materials.* 1994; 3: 902-911.
6. Hainsworth S V, Uhure N J. Diamond like carbon coating for Tribology: Production techniques, characterization, methods and applications. *International Material Reviews. 2007;* 52: 153-174.
7. Erdemir A, Donnet C. Tribology of diamond, diamond – like carbon, and related films. In: Modern Tribology Handbook, Bhusan, B. (Ed.), CRC press, New York. 2001; 871-905.
8. Vanhulsel A, Velasco F, Jacobs R, Eersels L, Havermans D, Roberts E W, Sherrington I, Anderson M J, Gaillard L. DLC solid lubricant coatings on ball bearings for space applications. *Tribology International.* 2007; 40: 1186-1194.
9. Leroy C, Schiffmann K I, van Acher K, von Stebut J. Ball cratering: an efficient tool for 3 body microabrasion of coated systems. *Surface and Coatings Technology.* 2005; 200: 153-156.

10. Podgornik B, Vižintin B, Ronkainen H, Holmberg K. Friction and wear properties of DLC-coated plasma nitrided steel in unidirectional and reciprocating sliding. *Thin Solid Films*. 2000; 377/378: 254-260.
11. Buchner B, Umgeher A, Buchmayr B. Estimation of friction under forging conditions by means of the ring on disc test. *Conference proceedings of American Institute of Physics.* 2007; 907: 505-508.
12. Bull S J. Tribology of carbon coatings: DLC, diamond and beyond. *Diamond and Related Materials.* 1995; 4: 827-836.
13. Dearnley G, Arps J H. Biomedical applications of diamond-like carbon (DLC) coatings: A review. *Surface and Coatings Technology.* 2005; 200: 2518-2524.
14. Thorwarth G, Falub C V, Műller U, Weisse B, Voisard C, Tobler M, Hauert R. Tribological behavior of DLC-coated articulating joint implants. *Acta Biomaterials.* 2010; 6: 2335-2341.
15. Dorner-Reisel A, Schurer C, Muller E. The wear resistance of diamond like carbon coated and uncoated Co28Cr6Mo knee prostheses. *Diamond and Related Materials.* 2004; 13: 823-827.
16. Saikko V, Ahlroos T, Calonius O, Keränen J. Wear simulation of total hip prostheses with polyethylene against CoCr, alumina and diamond-like carbon. *Biomaterials.* 2001: 22: 1507-1514.
17. Sheeja D, Tay B K, Nung L N. Feasibility of diamond-like carbon coatings for orthopaedic applications. *Diamond and Related Materials.* 2004; 13: 184-190.
18. Galvin A, Brockett C, Williams S, Hatto P, Burton A, Issac G, Stone M, Ingham E, Fisher J. Comparison of wear of ultra-high molecular weight polyethylene acetabular cups against surface-engineered femoral heads. *Proceedings of Institute of Mechanical Engineering, Part H*. 2008; 222: 1073-1080.

19. Xu T, Pruitt L. Diamond-like carbon coatings for orthopaedic applications: An evaluation of tribological performance. *Journal of Material Science: Material in Medicine.* 1999; 10: 83-90.
20. Dowling D P, Kola P V, Donnelly K, Kelly T C, Brumitt K, Lloyd L, Eloy R, Therin M, Weill N. Evaluation of diamond-like carbon, coated orthopaedic implants. *Diamond and Related Materials*. 1997; 6: 390-393.
21. Kim W, Kin J, Park S, Lee K. Tribological and electrochemical characteristics of DLC coatings with bias voltage. *Metallurgical and Materials International.* 2005; 11: 473-480.
22. Shi X, Wang Q, Xu L, Ge S, Wang C. Hydrogenated diamond-like carbon film deposited on UHMWPE by RF-PECVD. *Applied Surface Sciences*. 2009; 255: 8246-8251.
23. Puértolas J A, Martinez-Nogués V, Martinez-Morlanes M J, Mariscal M D, Medel F J, López-Santos C, Yubero F. Improved wear performance of ultra high molecular weight polyethylene coated with hydrogenated diamond like carbon. *Wear*. 2010; 269: 458-465.
24. Neuville S, Matthews A. A perspective on the optimization of hard carbon and related coatings for engineering applications. *Thin Solid Films.* 2007; 515: 6619-6653.
25. Dearnley P A, Neville A, Turner S, Scheibe H-J, Tietema R, Tap R, Stuber M, Hovsepian P, Layyous A, Stenbom B. Coatings tribology drivers for high density plasma technologies. *Surface Engineering*. 2010; 26: 80-96.
26. Klaffke D, Santner E, Spaltmann D, Woydt M. Influences on the tribological behavior of slip-rolling DLC coatings. *Wear*. 2005; 259: 752-758.

27. Peng X L, Clyne T W. Residual stress and debonding of DLC films in metallic substrate. *Diamond and Related Materials.* 1998; 7: 944-950.
28. Michler T, Grischke M, Traus I, Bewilogua K, Dimigen H. Mechanical properties of DLC films prepared by bipolar pulsed DC PACVD. *Diamond and Related Materials.* 1998; 7: 1333-1337.
29. Johnson K L. Contact Mechanics, the Press Syndicate of the University of Cambridge, Cambridge. 1985; 90-104: 56-63.
30. Gitis N V, Xiao J, Vonogradov M. Multi-sensor testing of thin and thick coatings for adhesion and delamination. *Proceedings of 26th Annual Meeting of the Adhesion Society*, Myrtle Beach, 133-135, February 2003.
31. Weiler M, Sattel S, Giessen T, Jung K, Ehrhardt H, Veerasamy V S, Robertson J. Preparation and properties of highly tetrahedral hydrogenated amorphous carbon. *Physical Review B.* 1996; 53: 1594-1609.
32. Gopinathan N, Robinson C, Ryan F. Characterization and properties of diamond-like carbon films for magnetic recording application. *Thin Solid Films*. 1999; 355-356: 401-405.
33. Steiner L, Bouvier V, May U, Hegadekatte V, Huber N. Modelling of unlubricated oscillating sliding wear of DLC-coatings considering surface topography, oxidation and graphitisation. *Wear*. 2010; 268: 1184-1194.
34. Mukhopadhyay S M. Chapter 9: Sample Preparation for Microscopic and Spectroscopic Characterization of Solid surfaces and films. In: Mitra S. Sample Preparation Techniques in Analytical Chemistry (Volume 162), A John Wiley and Sons, Inc., Publications, New Jersey. 2003; 377-411.

35. Ledrappier F, Langlade C, Gachon Y, Vannes B. Blistering and spalling of thin hard coatings submitted to repeated impacts. *Surface Coatings and Technology.* 2008; 202: 1789-1796.
36. Dearnley P A, Elwafi A M, Chittenden R J, Barton D C. Wear and friction of Diamond-like-carbon coated and uncoated steel roller bearings under high contact pressure oil lubricated rolling/sliding conditions. *Journal of Tribology*. 2014; 136: 021101-021111.
37. Suzuki M, Ohana T, Tanaka A. Tribological properties of DLC films with different hydrogen contents in water environment. *Diamond and Related Materials.* 2004; 2216-2220.
38. Gangopadhyay A, Sinha K, Uy D, McWatt D G, Zdrodowski R J, Simko, S J. Friction, wear and surface film formation characteristics of diamond-like carbon thin coating in valve-train application. *Tribology Transactions.* 2011; 54: 104-114.
39. Liu Y, Erdemir A, Meletis E I. A study of wear mechanism of diamond-like carbon films. *Surface Coating and Technology.* 1996; 82: 48-56.
40. Voevodin, A A, Phelps A W, Zabinski J S, Donley M S. Friction induced phase transformation of pulsed laser deposited diamond-like carbon. *Diamond and Related Materials.* 1996; 5: 1264-1269.
41. Sánchez-López J C, Erdemir A, Donnet C, Rojas T C. Friction-induced structural transformations of diamondlike carbon coatings under various atmospheres. *Surface coatings and Technology*. 2003; 163-164: 444-450.
42. Oguri K, Arai T. Friction coefficient of SiC, TiC and GeC coatings with excess Carbon formed by plasma-assisted chemical vapour deposition. *Thin Solid Films.* 1992; 208: 158–160.